

© 2016 IEEE. Personal use of this material is permitted. Permission from IEEE must be obtained for all other uses, in any current or future media, including reprinting/republishing this material for advertising or promotional purposes, creating new collective works, for resale or redistribution to servers or lists, or reuse of any copyrighted component of this work in other works.

Scattering from a cylindrical object of arbitrary cross section with the use of field matching method

Rafal Lech, *Member, IEEE*, Piotr Kowalczyk, Adam Kusiek, *Member, IEEE*

Abstract—A simple and intuitive solution to scattering problems in shielded and open structures is presented. The main idea of the analysis is based on the direct field matching technique involving the usage of projection of the fields at the boundary on a fixed set of orthogonal basis functions. Different convex shapes and various obstacle materials are considered to verify the validity of the method in open and closed structures. The results cohere with those obtained by commercial software.

Index Terms—Cylindrical structure, Field matching, Scattering.

I. INTRODUCTION

Scattering is one of the canonical problems of electromagnetic waves. Such issues are crucial to propagation analysis and the design of microwave and optical devices (e.g., shaping of radiation patterns, filters and circulators). The last century provided numerous analytical and numerical methods for addressing these problems.

In open space, for obstacles of cross sections that can be exactly described by constant coordinates of orthogonal systems, the direct field matching technique can be applied. Such an approach has been presented in numerous textbooks (e.g., for circular and elliptical rods [1]). This technique can be quite simple and has notably low numerical cost if the basis functions are correctly chosen. The problem becomes more difficult when complex obstacle shapes are considered. However, since the early 1970's, the integral equation method [2] has been developed and, today, almost any obstacle shape can be thereby examined. The introduction of electric and magnetic currents and application of the reciprocity theorem to the scattered fields can be found from Green's identity by using Green's function. This method quickly became popular and is commonly used to this day [3]–[8]. However, in the numerical analysis, the use of Green's function is often complicated due to the singular points in the computational domain [9].

In this paper, we present a simple and intuitive solution to the scattering problems in shielded and open areas. The main idea of the analysis is based on decomposition of the obstacles' fields into Fourier-Bessel series with unknown coefficients. The fields are then matched at the boundary using a projection of the fields on a fixed set of orthogonal basis functions. The different shapes of the obstacles do not complicate the analysis since the fields can be expressed in terms of tangential and

R. Lech, P. Kowalczyk and A. Kusiek are with the Department of Microwave and Antenna Engineering, Faculty of Electronics, Telecommunications and Informatics, Gdansk University of Technology, Gdansk, 80-233 Poland e-mail: rlech@eti.pg.gda.pl, pio.kow@gmail.com, adakus@eti.pg.gda.pl.

This work was supported from sources of National Science Center under grant decision no. DEC-2013/11/B/ST7/04309.

Manuscript received MMMM DD, 2014; revised MMMM DD, 2014.

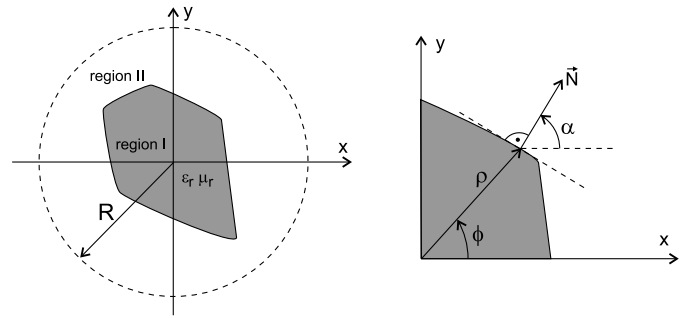


Fig. 1. The geometry of an investigated structure. The definition of angle α .

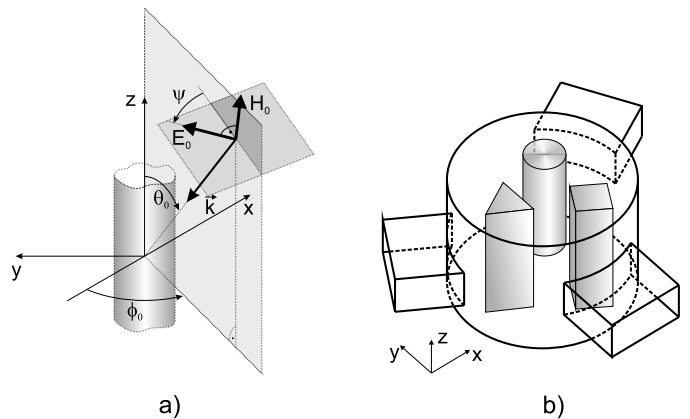


Fig. 2. Open and closed structures: a) plane wave illumination at arbitrary angle, b) waveguide junction.

transverse components. Such an approach does not require the use of currents and Green's function, and therefore its computation and implementation are much less complex.

In order to generalize the proposed technique, the scatterer is replaced by impedance matrix \mathbf{Z} , defined on a hypothetical circular cylinder. The impedance matrix represents a relation between the electric and magnetic fields of the abstract circular cylinder, independent of the incident field [10]. Such an approach allows for the analysis of scattering in different scenarios, e.g., in waveguides and resonators as well as in the open region. Moreover, such a technique facilitates multi-object scattering analysis and the interaction between the obstacles can be modeled using the iterative procedure [11].

All the obtained results have been verified by comparison with simulations performed using a finite element-based method [12], [13]. However, the efficiency of the discrete (even hybrid [14]) methods cannot be compared in the same way, due to the greatly differing approaches of the methods. The methods that discretize the computational domain are more general, though they are significantly more time and memory consuming, especially when dense meshes must be employed to model the complex shapes of the structures. By contrast, the dedicated methods, such as that proposed in this paper, are not as general but are much more suitable for utilization in the optimization process.

II. FORMULATION OF THE PROBLEM

The investigated structure is a cylindrical object of arbitrary convex cross section as illustrated in Fig. 1, which is assumed to be invariant along its axis. The problem of electromagnetic wave scattering is considered and the aim of the analysis is to determine the relation between the electric and magnetic fields on the surface of a hypothetical cylinder of radius R , which surrounds the structure (see Fig. 1). This relation can be expressed in the form of a multimode impedance matrix \mathbf{Z}_c , which describes the investigated structure. Obtaining the impedance matrix allows us to match it to any known external incident fields, as described in [10] and [11], and enables us to analyze a very wide class of closed and open structures, e.g., scattering from cylindrical objects located in free space and illuminated obliquely by a plane wave, or located in multipoint waveguide junctions and excited from the waveguide ports, as presented in Fig. 2. As the angle of incidence of a plane wave may be arbitrary and the waveguides exciting the junction may have different heights, the analyzed problem can be classified as 2.5 D.

Two regions of investigation can be distinguished in the structure: region I, located inside the object, and region II, outside. Region II is bounded by the assumed hypothetical cylinder of radius R . The z components of the electric and magnetic fields in both regions have the following form (suppressing $e^{j\omega t}$ time dependence):

$$F_z^I = \sum_{n=0}^N \sum_{m=-M}^M A_{n,m}^F Z_m^I(k_{\rho n}^I) e^{jm\phi} f^F(k_{zn}z) \quad (1)$$

$$F_z^{II} = \sum_{l=1}^2 \sum_{n=0}^N \sum_{m=-M}^M B_{l,n,m}^F Z_m^l(k_{\rho n}^{II}) e^{jm\phi} f^F(k_{zn}z) \quad (2)$$

where $F = \{E, H\}$, $k_{\rho n}^i = \sqrt{\omega^2 \mu_i \varepsilon_i - k_{zn}^2}$ for $i = \{I, II\}$, ω is the angular frequency, $Z_m^I(\cdot)$ is a Bessel function of order m and $Z_m^2(\cdot)$ is a Hankel function of the second kind and order m . The utilization of the Hankel function of the second kind satisfies Sommerfeld's radiation condition (representing the outward-traveling wave). Due to the assumed field representation in (1) and (2), only convex obstacle shapes can be analyzed. Functions f^E , f^H and wave number k_{zn} depend on boundary conditions defined above and below the structure. Placing the structure in the rectangular waveguide junction of height b , these functions take the form:

$$f^E(k_{zn}z) = \cos(k_{zn}z), \quad f^H(k_{zn}z) = \sin(k_{zn}z) \quad (3)$$

where $k_{zn} = n\pi/b$. In the case of plane wave scattering on the investigated object, which is infinitely long:

$$f^{E,H}(k_z z) = e^{jk_z z} \quad (4)$$

where $k_z = k_0 \cos(\theta_0)$, k_0 is a wavenumber of free space and θ_0 is an angle of plane wave incidence, defined with respect to the z -axis. In this case the summation over n in (1) and (2) vanishes. The other components of the electric and magnetic fields (E_ϕ , E_ρ , H_ϕ and H_ρ) can be derived from Maxwell's equations, as in [15].

In order to determine the impedance matrix \mathbf{Z}_c on the contours of the outer cylinder of radius R , we utilize the

field matching method. First, the continuity conditions for the tangential field components on the surface of the investigated object must be satisfied. As we have assumed the lateral surface of the cylinder is invariant of z and is of arbitrary cross section, it can thus be described by functions $\rho = \varrho(s)$ and $\phi = \varphi(s)$, where s is the curvilinear coordinate that follows the surface. Hence, the continuity conditions must be fulfilled for arbitrary z and any s from 0 to the total length S of the boundary:

$$F_z^I(\varrho(s), \varphi(s), z) = F_z^{II}(\varrho(s), \varphi(s), z) \quad (5)$$

$$F_t^I(\varrho(s), \varphi(s), z) = F_t^{II}(\varrho(s), \varphi(s), z) \quad (6)$$

where

$$F_t^{(\cdot)}(\cdot) = C_\rho(s) F_\rho^{(\cdot)}(\cdot) + C_\phi(s) F_\phi^{(\cdot)}(\cdot) \quad (7)$$

with

$$C_\rho(s) = \sin \varphi \cos \alpha - \cos \varphi \sin \alpha \quad (8)$$

$$C_\phi(s) = \cos \varphi \cos \alpha + \sin \varphi \sin \alpha \quad (9)$$

where $\alpha = \alpha(s)$ is an angle between the x -axis and the normal outgoing vector \vec{N} to the cylinder surface (see Fig. 1). For instance, for the cylinder of circular cross section $\alpha = \phi$ on each point of the surface.

For equations (5) and (6) a projection on the orthogonal set of the functions:

$$w_p(s) = \frac{1}{\sqrt{S}} \exp\left(\frac{j2\pi p}{S}s\right) \quad (10)$$

for ($p = -M \dots M$) can be applied in the meaning of the inner product:

$$\langle g | w_p \rangle = \int_0^S g(s) w_p(s)^* ds \quad (11)$$

Combining the electric field components in one matrix equation and the magnetic field components in another, we obtain the following set:

$$\mathbf{M}_1^{E,I} \mathbf{A} = \mathbf{M}_1^{E,II} \mathbf{B}_1 + \mathbf{M}_2^{E,II} \mathbf{B}_2 \quad (12)$$

$$\mathbf{M}_1^{H,I} \mathbf{A} = \mathbf{M}_1^{H,II} \mathbf{B}_1 + \mathbf{M}_2^{H,II} \mathbf{B}_2 \quad (13)$$

where $\mathbf{B}_l = [\mathbf{B}_l^E, \mathbf{B}_l^H]^T$, $\mathbf{A} = [\mathbf{A}^E, \mathbf{A}^H]^T$, with $\mathbf{B}_l^F = [B_{l,0,-M}^F, \dots, B_{l,N,M}^F]^T$ and $\mathbf{A}^F = [A_{l,0,-M}^F, \dots, A_{l,N,M}^F]^T$, and matrices $\mathbf{M}_l^{F,i}$ have the form:

$$\mathbf{M}_l^{E,i} = \begin{bmatrix} \mathbf{M}_{l,z}^{E,i} & \mathbf{0} \\ \mathbf{M}_{l,t1}^{E,i} & \mathbf{M}_{l,t2}^{E,i} \end{bmatrix}, \quad \mathbf{M}_l^{H,i} = \begin{bmatrix} \mathbf{M}_{l,t1}^{H,i} & \mathbf{M}_{l,t2}^{H,i} \\ \mathbf{0} & \mathbf{M}_{l,z}^{H,i} \end{bmatrix} \quad (14)$$

where the submatrices $\mathbf{M}_{l,(\cdot)}^{F,i}$ are block diagonal with respect to n number and their elements have the following form:

$$\{\mathbf{M}_{l,z}^{F,i}\}_{m,p} = \langle \mathcal{Z}_{mn}^{l,i} | w_p \rangle$$

$$\{\mathbf{M}_{l,t1}^{E,i}\}_{m,p} = \langle C_\rho \zeta_\rho^e \mathcal{Z}_{mn}^{l,i} + C_\phi \zeta_\phi^e \mathcal{Z}_{mn}^{l,i} | w_p \rangle$$

$$\{\mathbf{M}_{l,t2}^{E,i}\}_{m,p} = \langle C_\rho \zeta_\rho^h \mathcal{Z}_{mn}^{l,i} + C_\phi \zeta_\phi^h \mathcal{Z}_{mn}^{l,i} | w_p \rangle$$

$$\{\mathbf{M}_{l,t1}^{H,i}\}_{m,p} = \langle C_\rho \zeta_\rho^e \mathcal{Z}_{mn}^{l,i} + C_\phi \zeta_\phi^e \mathcal{Z}_{mn}^{l,i} | w_p \rangle$$

$$\{\mathbf{M}_{l,t2}^{H,i}\}_{m,p} = \langle C_\rho \zeta_\rho^h \mathcal{Z}_{mn}^{l,i} + C_\phi \zeta_\phi^h \mathcal{Z}_{mn}^{l,i} | w_p \rangle$$

where $Z_{mn}^{l,i} = Z_m^l(k_{\rho n}^i \rho) e^{jm\varphi}$, prime denotes derivative of the function and ζ and ξ are the proper field coefficients. For the case of plane wave scattering on the investigated object, these coefficients are as follows:

$$\begin{aligned} \zeta_\rho^e &= \frac{jk_z}{k_\rho}, & \zeta_\phi^e &= \frac{-k_z m}{k_\rho^2 \rho}, & \zeta_\rho^h &= \frac{\omega \mu m}{k_\rho^2 \rho}, & \zeta_\phi^h &= \frac{j\omega \mu}{k_\rho}, \\ \xi_\rho^e &= \frac{-\omega \varepsilon m}{k_\rho^2 \rho}, & \xi_\phi^e &= \frac{-j\omega \varepsilon}{k_\rho}, & \xi_\rho^h &= \frac{jk_z}{k_\rho}, & \xi_\phi^h &= \frac{-k_z m}{k_\rho^2 \rho}. \end{aligned}$$

Eliminating the unknown coefficients \mathbf{A} of the fields in region I, we can relate the coefficients in region II as follows:

$$\mathbf{B}_2 = \mathbf{T} \mathbf{B}_1 \quad (15)$$

where

$$\mathbf{T} = \left(\mathbf{M}_2^{E,II} - \mathbf{Z}_0 \mathbf{M}_2^{H,II} \right)^{-1} \left(\mathbf{Z}_0 \mathbf{M}_1^{H,II} - \mathbf{M}_1^{E,II} \right) \quad (16)$$

with

$$\mathbf{Z}_0 = \mathbf{M}_1^{E,I} \left(\mathbf{M}_1^{H,I} \right)^{-1} \quad (17)$$

Only for a cylinder of a circular cross section are the submatrices $\mathbf{M}_{l,(\cdot)}^{F,i}$ diagonal and composed of appropriate Bessel or Hankel functions, or their derivatives with proper coefficients. For any other cylinder shape, the matrices can be full and it is necessary to perform $(N+1) \times (2M+1) \times (2M+1)$ integrations to calculate their values. It is also worth noting that, for an object made of PEC material, the \mathbf{Z}_0 matrix equals zero.

Utilizing the relation (15) between the coefficients in region II, it is possible to write the relation between the total electric and magnetic fields on the contour of the outer cylinder of radius R . This relation is described by the impedance matrix \mathbf{Z}_c and has the following form:

$$\mathbf{Z}_c = \left(\mathbf{N}_1^{E,II} + \mathbf{N}_2^{E,II} \mathbf{T} \right) \left(\mathbf{N}_1^{H,II} + \mathbf{N}_2^{H,II} \mathbf{T} \right)^{-1} \quad (18)$$

where

$$\mathbf{N}_l^{E,II} = \begin{bmatrix} \mathbf{N}_{l,z}^{E,II} & \mathbf{0} \\ \mathbf{N}_{l,\phi 1}^{E,II} & \mathbf{N}_{l,\phi 2}^{E,II} \end{bmatrix}, \quad \mathbf{N}_l^{H,II} = \begin{bmatrix} \mathbf{N}_{l,\phi 1}^{H,II} & \mathbf{N}_{l,\phi 2}^{H,II} \\ \mathbf{0} & \mathbf{N}_{l,z}^{H,II} \end{bmatrix} \quad (19)$$

where the submatrices $\mathbf{N}_{l,(\cdot)}^{F,II}$ are block diagonal with respect to n number and have the following form:

$$\begin{aligned} \{\mathbf{N}_{l,z}^{F,II}\}^n &= \text{diag} \left(Z_m^l(k_{\rho n}^{II} R) \right)_{m=-M}^M \\ \{\mathbf{N}_{l,\phi 1}^{E,II}\}^n &= \text{diag} \left(x_\phi^e Z_m^l(k_{\rho n}^{II} R) \right)_{m=-M}^M \\ \{\mathbf{N}_{l,\phi 2}^{E,II}\}^n &= \text{diag} \left(x_\phi^h Z_m^l(k_{\rho n}^{II} R) \right)_{m=-M}^M \\ \{\mathbf{N}_{l,\phi 1}^{H,II}\}^n &= \text{diag} \left(y_\phi^e Z_m^l(k_{\rho n}^{II} R) \right)_{m=-M}^M \\ \{\mathbf{N}_{l,\phi 2}^{H,II}\}^n &= \text{diag} \left(y_\phi^h Z_m^l(k_{\rho n}^{II} R) \right)_{m=-M}^M \end{aligned}$$

where $\text{diag}(\cdot)_m$ denotes a diagonal matrix with respect to m .

In open space, the presented approach seems to be equivalent to the classical integral equation method [2] – Green's function is represented by a Hankel function, currents correspond to the fixed orthogonal basis and integration is performed over the boundary of the obstacle. However, in the

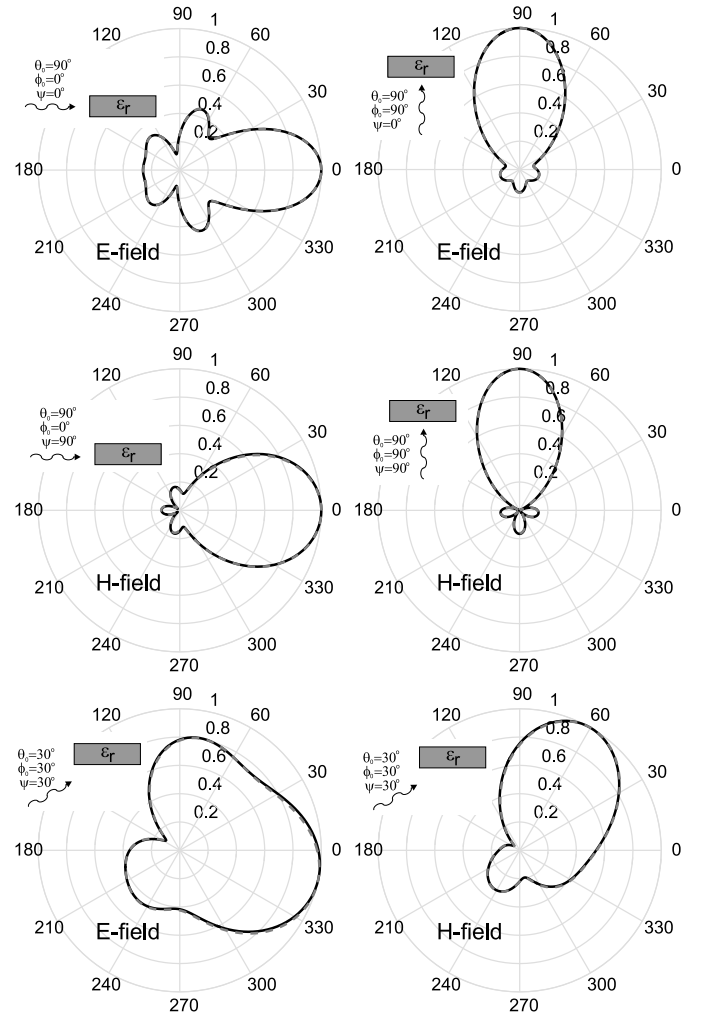


Fig. 3. Normalized amplitude of scattered electric and magnetic fields from the dielectric ($\varepsilon_r = 5$) rectangular cylinder with dimensions $1\lambda \times 0.25\lambda$ for different angles of plane wave incidence. Solid line - this method, dashed line - HFSS.

presented technique, integration of a Hankel function does not involve singularities, which is beneficial from a computational point of view.

III. RESULTS

In order to verify the validity of the presented approach, a few examples of electromagnetic field scattering in different scenarios have been analyzed. Utilizing the calculated impedance matrix describing the analyzed object, it is possible to apply external excitation. Assuming the plane wave illumination at an arbitrary angle of incidence, as illustrated in Fig. 2(a), we can calculate the scattered field in the far zone. We can also place the investigated object in a multiport waveguide junction, as illustrated in Fig. 2(b), and calculate the multimode scattering matrix of the junction.

In the first example, a plane wave scattering from a dielectric cylinder of rectangular cross section is considered. The cylinder has dimensions $1\lambda \times 0.25\lambda$ and is made of dielectric with $\varepsilon_r = 5$. The vertices of the rectangle are rounded (with a radius equal to the tenth part of the shorter edge). Several cases

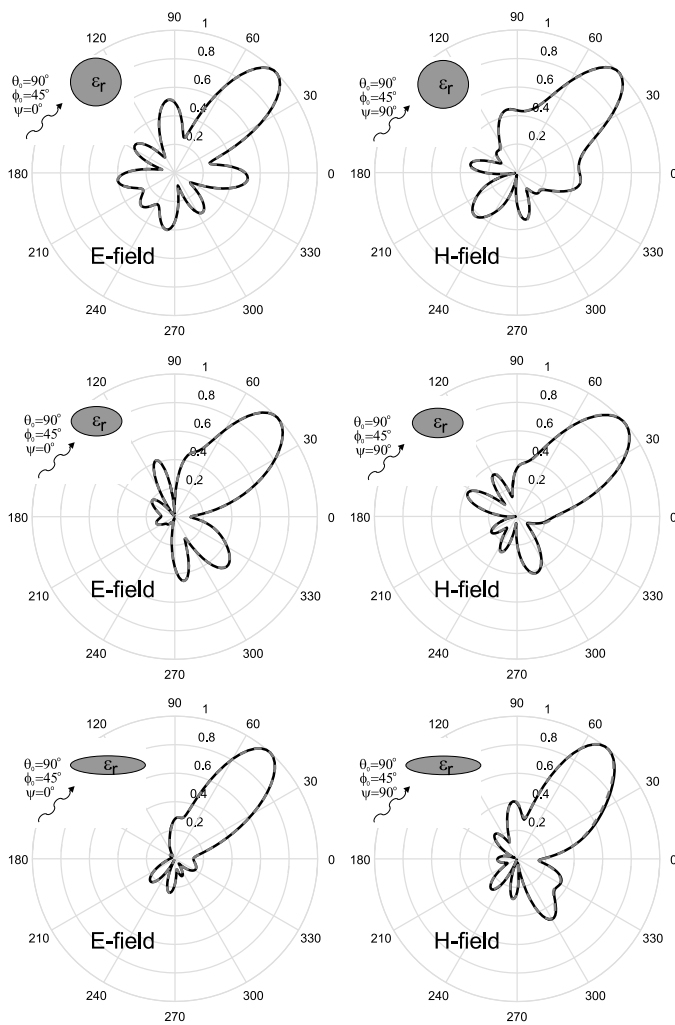


Fig. 4. Normalized amplitude of scattered electric and magnetic fields from the dielectric ($\epsilon_r = 5$) elliptical cylinder, for plane wave incidence angle $\theta_0 = 90^\circ$, $\phi_0 = 45^\circ$, with the following dimensions: first row $0.75\lambda \times 0.75\lambda$, second row $1\lambda \times 0.5\lambda$ and third row $1\lambda \times 0.25\lambda$. Solid line - this method, dashed line - HFSS.

of plane wave illuminations are considered and the results are presented in Fig. 3. In the case of perpendicular excitation ($\theta_0 = 90^\circ$), the TE^z and TM^z solutions are uncoupled and can therefore be considered separately. Specifically, for the angle $\psi = 0^\circ$, only the E_z , H_ϕ and H_ρ field components exist, while, for the angle $\psi = 90^\circ$, there are only H_z , E_ϕ and E_ρ components. When $\theta_0 \neq 90^\circ$, both solutions are coupled and all field components must be taken into consideration. For the presented structure, it was sufficient to select $M = 25$ mode expansion functions and the integrals in (14) were evaluated with the use of the trapezoidal rule, with $P = 492$ points evenly covering the boundary. The obtained results are compared with the calculations of the HFSS commercial simulator, obtaining good agreement.

The convergence of the method is shown in Table I for the last case of plane wave illumination. The following definition

TABLE I
CONVERGENCE OF THE METHOD FOR THE EXAMPLE FROM FIG. 3. UPPER VALES - E FIELD, LOWER VALUES (IN BRACKETS) - H FIELD.

M	$P = 124$	$P = 246$	$P = 492$	$P = 984$
5	0.0483 (0.2400)	0.0472 (0.2400)	0.0469 (0.2400)	0.0468 (0.2400)
10	0.0168 (0.0933)	0.0170 (0.0919)	0.0172 (0.0917)	0.0172 (0.0917)
15	14.1300 (14.9000)	0.0115 (0.0727)	0.0116 (0.0726)	0.0116 (0.0725)
20	45.7900 (107.3800)	0.0095 (0.0626)	0.0096 (0.0624)	0.0096 (0.0624)
25	24.7700 (21.5500)	0.9300 (0.7100)	0.0070 (0.0573)	0 (0)

of the error is assumed:

$$Err^{(M,P)} = \frac{\int_0^{2\pi} (F^{(M,P)}(\phi) - F^{(M_R,P_R)}(\phi))^2 d\phi}{\int_0^{2\pi} (F^{(M_R,P_R)}(\phi))^2 d\phi} \cdot 100\% \quad (20)$$

where F is the magnitude of the electric or magnetic fields in the far zone $\rho = 100\lambda$, $M_R = 25$ and $P_R = 984$. As can be observed, the utilization of $P = 492$ discretization points is sufficient to obtain accurate results, however, the number of modes should not be less than $M = 25$.

In the second example, a plane wave scattering from a cylinder of elliptical cross section is considered. Only the perpendicular case is considered ($\theta_0 = 90^\circ$) with the plane wave illuminating the object from a $\phi_0 = 45^\circ$ angle. Three ellipse shapes are considered: a circular cross section with axes dimensions $0.75\lambda \times 0.75\lambda$, an elliptical cross section with axes dimensions $1\lambda \times 0.5\lambda$ and another elliptical cross section with axes dimensions $1\lambda \times 0.25\lambda$. For the presented structure, it was sufficient to select $M = 25$ mode expansion functions and the integrals in (14) were evaluated with the use of the trapezoidal rule with $P = 360$ points. The obtained results (shown in Fig. 4) are also compared with the calculations of the HFSS commercial simulator and again good agreement is achieved.

In the third example, a ferrite cylinder of triangular cross section (the vertexes of the triangle are rounded), placed in the cylindrical metallic enclosure and fed by three rectangular waveguides, is investigated. The WR-90 waveguides with dimensions $a = 22.86$ mm and $b = 10.16$ mm are used. The metallic enclosure has the same height as the waveguides and a radius $R = a/\sqrt{2}$. The waveguides are evenly located along the ϕ direction, as presented in Fig. 5. The triangular ferrite cylinder presents dimensions $a = 10$ mm (equilateral) and completely fills the height of the waveguide junction. The ferrite material, magnetized along z -axis, is used with internal bias magnetic field intensity $H_i = 80$ kA/m and saturated magnetization $M_s = -150$ kA/m. The calculated scattering parameters of the junction are presented in Fig. 5. Due to the symmetry of the structure, only S_{11} , S_{21} and S_{31} are shown. For the presented structure it was sufficient to select $M = 10$ mode expansion functions and the integrals in

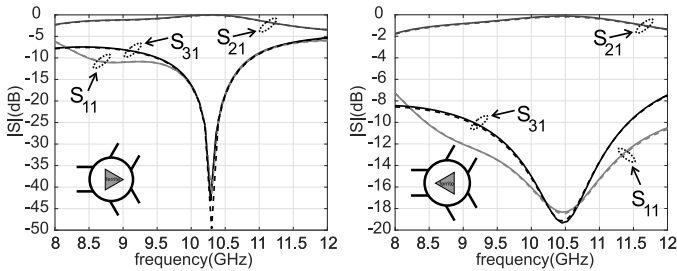


Fig. 5. Scattering parameters of the three-port waveguide junction (WR-90 waveguide) with triangular ferrite cylinder of dimensions $a = 10$ mm (equilateral triangle) and ferrite material parameters: $\epsilon_r = 8$, $H_i = 80$ kA/m and $M_s = -150$ kA/m. Solid line - this method, dashed line - HFSS.

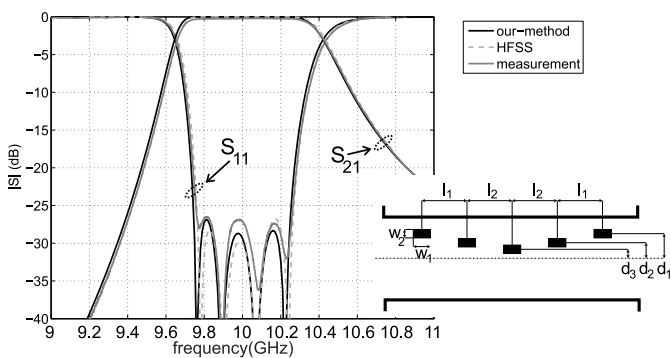


Fig. 6. Scattering parameters of the four-pole filter. Dimensions: $w_1 = 6$ mm, $w_2 = 3$ mm, $l_1 = 18.31$ mm, $l_2 = 21.31$ mm, $d_1 = 2.27$ mm, $d_2 = 3.00$ mm, $d_3 = 5.76$ mm; height of the posts $h = 10.16$ mm.

(14) were evaluated with the use of the trapezoidal rule with $P = 279$ points. The obtained results are again compared with the calculations of the HFSS commercial simulator and good agreement is found.

In the last example, a waveguide filter employing five metallic posts of rectangular cross section is considered [16]. Again the WR-90 waveguide is used. Its dimensions and the obtained results are presented in Fig. 6. For the presented structure it was sufficient to select $M = 10$ mode expansion functions and the integrals in (14) were evaluated with the use of the trapezoidal rule with $P = 300$ points, which were evenly distributed along the contour of the object. The obtained results are compared with the calculations of the HFSS commercial simulator and measurement results from [16], again obtaining good agreement.

The calculations were performed in a Matlab environment on an Intel Xenon X5690 3.47 GHz (2 processors). For the assumed number of mode expansions and integration points, the calculation of a single frequency point took approximately 1.2 s for the first example, 0.9 s for the second example and 0.15 s for the third and final examples. Comparing this to the calculation of the commercial software, ANSYS HFSS, the calculation time of a single frequency point took 160 s for an open structure (first example – 94127 tetrahedra) and 5 min for a closed structure (third example – 45310 tetrahedra). The developed model is dedicated only to the structures considered in this article, and therefore the difference between the effectiveness of our method with respect to HFSS is not

surprising. Nevertheless, these results clearly show that such a model is suitable for utilization in the optimization process.

IV. CONCLUSION

The field matching technique presented in this article is simple and effective. The direct implementation and low numerical cost result in fast calculations. Its efficiency has been verified on a number of open and closed structures and the results are in good agreement with a finite element-based method (commercial software).

REFERENCES

- [1] L. Tsang, J. A. Kong, K.-H. Ding, *Scattering of Electromagnetic Waves: Theories and Applications*, John Wiley and Sons, Inc., 2002.
- [2] Okamoto, Naomichi, "Matrix formulation of scattering by a homogeneous gyrotropic cylinder," *IEEE Transactions on Antennas and Propagation*, vol. 18, no. 5, pp. 642–649, Sep. 1970.
- [3] G.P. Zouros, G.C. Kokkorakis, "Electromagnetic Scattering by an Inhomogeneous Gyroelectric Sphere Using Volume Integral Equation and Orthogonal Dini-Type Basis Functions," *IEEE Transactions on Antennas and Propagation*, vol. 63, no. 6, pp.2665–2676, June 2015.
- [4] Libo Wang, Lianlin Li, Yunhua Tan, "A Novel Approximate Solution for Electromagnetic Scattering by Dielectric Disks," *IEEE Transactions on Geoscience and Remote Sensing*, vol. 53, no. 5, pp. 2948–2955, May 2015.
- [5] F.D. Quesada Pereira, A. Romera Perez, P. Vera Castejon, A. Alvarez Melcon, "Integral-Equation Formulation for the Analysis of Capacitive Waveguide Filters Containing Dielectric and Metallic Arbitrarily Shaped Objects and Novel Applications," *IEEE Transactions on Microwave Theory and Techniques*, vol. 63, no. 12, pp. 3862–3873, Dec. 2015.
- [6] Y. Brick, V. Lomakin, A. Boag, "Fast Green's Function Evaluation for Sources and Observers Near Smooth Convex Bodies," *IEEE Transactions on Antennas and Propagation*, vol. 62, no. 6, pp.3374–3378, June 2014.
- [7] A. Aydogan, F. Akleman, "Analysis of Direct and Inverse Problems Related to Circular Waveguides Loaded With Inhomogeneous Lossy Dielectric Objects," *IEEE Transactions on Microwave Theory and Techniques*, vol. 62, no. 6, pp. 1291–1300, June 2014.
- [8] Y. Okuno and K. Yasuura, "Numerical algorithm based on the mode-matching method with a singular-smoothing procedure for analyzing edge-type scattering problems," *IEEE Transactions on Antennas and Propagation*, vol. 30, no. 4, pp. 580–587, Jul 1982.
- [9] W.C. Gibson, *The Method of Moments in Electromagnetics* CRC Press Taylor and Francis Group, 2015.
- [10] M. Polewski and J. Mazur, "Scattering by an Array of Conducting, Lossy Dielectric, Ferrite and Pseudochiral Cylinders," *Progress In Electromagnetics Research*, Vol. 38, pp. 283–310, 2002.
- [11] M. Polewski, R. Lech, J. Mazur, "Rigorous modal analysis of structures containing inhomogeneous dielectric cylinders," *IEEE Transactions on Microwave Theory and Techniques*, vol. 52, no. 5, pp. 1508–1516, May 2004.
- [12] G. Fotyga, M. Rewienski, M. Mrozowski, "Wideband Macromodels in Finite Element Method," *IEEE Microwave and Wireless Components Letters*, vol. 25, no. 12, pp.766–768, Dec. 2015.
- [13] HFSS Manual, www.ansys.com/Products/Electronics/ANSYS-HFSS
- [14] A. Kusiek, R. Lech, J. Mazur, "A New Hybrid Method for Analysis of Scattering From Arbitrary Configuration of Cylindrical Objects," *IEEE Transactions on Antennas and Propagation*, vol. 56, no. 6, pp. 1725–1733, June 2008.
- [15] D. M. Pozar, *Microwave Engineering, 4th Edition*, Reading, MA: Addison-Wesley 2012.
- [16] R. Lech, A. Kusiek, J. Mazur, "Tuning Properties of Irregular Posts in Waveguide Junction - Tunable Filter Application," *18th International Conference on Microwave, Radar and Wireless Communications MIKON-2010*, Lithuania, Vilnius, 14-16 June 2010, pp. 705-708.